Pattern Recognition Vol. 13, No. 2, pp. 177–187, 1981
Printed in Great Britain.

0031-3203/81/020177-11 $02.00/0
Pergamon Press Ltd.

844

LOCAL IMAGE TRANSFORMATION: AN APPLICATION IN BIOLOGICAL ELECTRON MICROSCOPY

A. FAVRE, HJ. KELLER*
Institute of Anatomy, University of Berne, Buhlstrasse 26, CH-3012, Berne, Switzerland

(*Received* 28 *November* 1979; *in revised form* 28 *July* 1980; *received for publication* 19 *August* 1980)

Abstract—Local image transformation as well as the optimisation of their relevant parameters are presented in a supervised learning scheme for the automated detection of mitochondria in electron microscopic sections of the liver cell.

Simulation Texture Local operations Error of Bayes Covariogram.

INTRODUCTION

One of the main standing problems limiting the general use of automatic image analysis is the correct detection of objects, i.e. the exact allocation of each pixel (picture element) either to the background or to the object of interest as defined by the observer.

In biological electron microscopy the stains commonly used bind more or less to chemical compounds rather than being specific for exactly one of the components of interest. Detection based on grey levels usually fails, calling for more information from the local neighbourhood in order to achieve a correct segmentation.

In view of the existing discrimination module of our system, we shall consider image transformations yielding to a good object definition upon thresholding.

Hardware and time considerations restrict the choice of these operations: we only consider those local transformations which may be implemented in an on-line pre-processor. The method of estimation is not unique but depends on the geometrical shape of the objects considered so that two different criteria will be given.

Biologists' strong interest in mitochondria (see Fig. 1) influenced our choice of examples. (These organelles furnish the energy for metabolic processes within cells.) We achieved detection of whole mitochondrial sections and of their internal membranes (called cristae) with low error rates on a test set of images.

INSTRUMENTATION

The major hardware components of our system are a Quantimet 720 (QTM) image analyser (Cambridge Instruments) interfaced to a PDP 11/10. The QTM is a modular hardware system for image analysis with the following capabilities.

(a) Acquisition of pictures from a TV camera and Analog/Digital converter.
(b) Thresholding to obtain a binary image.
(c) Optional modification of the binary picture using shrink and expand transformations.[1]
(d) Evaluations of geometric features (such as area, perimeter, projections, etc.) either for the whole field or for each individual object.
(e) Transfer of the feature parameters by DMA into the PDP for further calculations.

All these operations are realised by hardware modules in real time, i.e. processing is done synchronously with one TV scan in 0.1 s.

The necessity for iterative transformations has resulted in the acquisition of an image store featuring 8 bits per pixel, read-modify-write operations at scan rate and an asynchronous I/O port to the minicomputer. Together with our processor under construction, the image store will be placed between the Analog/Digital converter and the thresholding module with a feedback path allowing iterative transformations.

LOCAL TRANSFORMS AND THEIR EXPRESSION

Numerous local transformations are used in image processing, some on digitized grey tone images as the Robert's cross-operator,[2] local means[3, 4, 5] and Haralick transform[6]; others are applied to binary images as masks,[7] line connections[5] etc.

A simple notation facilitates the formulation and manipulation of expressions in local transforms: the local operator calculates a new value for a central pixel

* This work has been supported by the Swiss National Science Foundation, grant 3.209.77 and reports a thesis submitted to the University of Neuchâtel.

from grey values of neighbouring pixels, the same operation being applied for each point of the whole picture (except on boundary conditions). This suggests the introduction of local co-ordinates with values (0,0) for the center point and offsets for neighbouring pixels. The value of the image function at offset (i,j) is denoted by $[i,j]$

Example. 1. The cross-operator H is usually expressed as:

$$H = |g(i+1,j+1) - g(i,j)| + |g(i+1,j) - g(i,j+1)|.$$

With the proposed notation this can be written as follows:

$$H = |[1,1] - [0,0]| + |[1,0] - [0,1]|.$$

2. The identity transform would be $[0,0]$.

The offsets within square brackets contain the geometric aspect of the transformations. We use them as elements of a special image processing language in our simulations.

We may consider affine modifications of expressions with offsets.

Let M be a 2×2 matrix, b be a vector, fixed x be any offset and let us denote

$$A(M,b)x = Mx + b.$$

A given expression E is calculated by using grey levels $[i,j]$ of points $(i,j)^t$, (the superscript t means transposition) expressed in local co-ordinates. We extend the application of $A(M, b)$ to an expression E so that $A(M,b)E$ is the result of the same calculations based on points $A(M,b)\,(i,j)^t$ instead of $(i,j)^t$.

Example. Let

$$I = \begin{pmatrix} 1 & 0 \\ 0 & 1 \end{pmatrix}, \quad R = \begin{pmatrix} 0 & 1 \\ 1 & 0 \end{pmatrix}, \quad Q = \begin{pmatrix} -1 & 0 \\ 0 & -1 \end{pmatrix}$$

$$E = |[0,1] - [0,0]|.$$

We have

$$A(I,0)E = |[0,1] - [0,0]|$$
$$A(R,0)E = |[1,0] - [0,0]|$$
$$A(Q,0)E = |[0,-1] - [0,0]|$$
$$A(R,0)A(Q,0)E = |[-1,0] - [0,0]| = A(RQ,0)E.$$

Now write the macro-expression:

$$G = A(I+R,0)A(I+Q,0)E = A(I,0)E + A(R,0)E + A(Q,0)E + A(RQ,0)E.$$

Using

$$D(h) = \begin{pmatrix} h & 0 \\ 0 & h \end{pmatrix}$$

we can define a family of expressions;

$$G(h) = A(D(h),0)G \qquad (1)$$

which is shorthand for

$$G(h) = |[0,0] - [0,h]| + |[0,0] - [0,h]| + |[0,0] - [h,0]| + |[0,0] - [-h,0]|.$$

In this way, modifying the parameter h in $D(h)$, we obtain the text of a new expression. If smoothing the result of $G(h)$ is required one needs only to sum up several translated expressions $G(h)$.

As before let us put $E = |[0,1] - [0,0]|$, the translated E by $b_k = (x_k, y_k)^t$ will be

$$A(I,b_k)E = |[x_k, 1+y_k] - [x_k, y_k]|.$$

In the same way, it is possible to consider

$$A(I,b_k)G(h)$$

and to define

$$SG(b) = \sum_{k=1}^{n} A(I,b_k)G(h),$$

where SG is the smoothed transform G.

QUALITY CRITERIA

Image transforms are selected by the quality of the resulting classification of the pixels, i.e. by object detection. This can only be assessed by comparing the results of the automatic detection with the drawing of a specialist.

It is important to adapt these criteria to the geometrical aspect of the objects. Let S_c be the set of points detected by the algorithm, S_t be the set of points drawn by the specialist (true object), $A(S_c)$, $A(S_t)$ be the corresponding areas and $L(S_t)$, $L(S_c)$ their boundary length.

First we can use the confusion matrix for giving an error, evaluated by:

$$A(S_t \cap \bar{S}_c) \quad \text{and} \quad A(\bar{S}_t \cap S_c)$$

where $\bar{S}$ is the complement of S in the picture. The Bayesian error,[8] B, can be expressed as follows;

$$B = [A(S_t \cap \bar{S}_c) + A(\bar{S}_t \cap S_c)]/\tilde{A}$$

where $\tilde{A}$ is the total area of the picture. This criterion fails if $A(S_t)$ is very small (e.g. stripe-like features). We have approximately:

$$B \simeq A(\bar{S}_t \cap S_c)/\tilde{A}.$$

Therefore, $S_c = \phi$ is a good but practically useless estimation of the objects. A practical example of this is furnished by the membranes which appear as black lines a few pixels wide on the pictures; more generally, we can think of objects with a high form factor:

$$[L(S_t)]^2/A(S_t) \gg 4\pi.$$

This suggested a different quality criterion.

Some practical problems must be solved: firstly it is difficult to draw one line upon another using a light pen on a screen. Secondly the intersection between the two lines will always be very small though the

maximum distance between them remains small. Expanding[1] one line results in partially covering the other. These hints lead us to the following formulae.

Let $d(S_c)$ be the expanding of S_c; we define $L[S_t \cap \overline{d(S_c)}]/L(S_t)$ as the proportion of boundary length of the *undetected* part, $L[S_t \cap d(S_c)]/L(S_t)$ as the proportion of boundary length of the part detected *correctly*, and $L(S_t) - L[S_t \cap d(S_c)]/L(S_t)$ as the proportion of boundary length of the part detected *incorrectly*.

RESULTS

Detection of mitochondria in the liver cell by grey-level discrimination leads to intolerable errors. We now indicate a series of pre-processing transformations which reduce these errors. Furthermore we indicate a technique for detecting cristae. Among the known algorithms we have used local line detection[9] and texture analysis.[4]

(a) *Learning the good transformation*

First, we worked on micrographs with known partition into mitochondria and background. This allowed us to estimate conditional distributions for a given transform and to determine the associate error of Bayes. Grey level distributions observed on these pictures have shown similar mean values. Hence local estimation of this quantity would result in a bad discriminant function. On the other hand local variation of the grey levels was smaller on mitochondria than on the background, as can be seen in Fig. 1. This variation could therefore result in good discriminant function.

We tried several formulae to enhance this texture. The most simple we found that gives a good estimation of local grey-level variation was the transformation $G(h)$ given in equation (1). Using the covariograms

$$J(h) = 1/2E[([0,h] - [0,0])^2]$$

we found an optimum value of h and at the same time confirmed the isotropy of the texture:

$$J(h) = J(\|h\|).$$

$\|h\| = 6$ pixels was the smallest value for which we obtained roughly the asymptotic difference between the 2 covariograms (Fig. 2). On average, this indicates the best sampling distance of the grey values in $G(h)$. The results obtained by $G(h)$ transform on the learning set shown that the conditional distributions are very similar (Fig. 3) and quite independent of the initial grey-level distributions.

After examination of the image transformed by $G(h)$

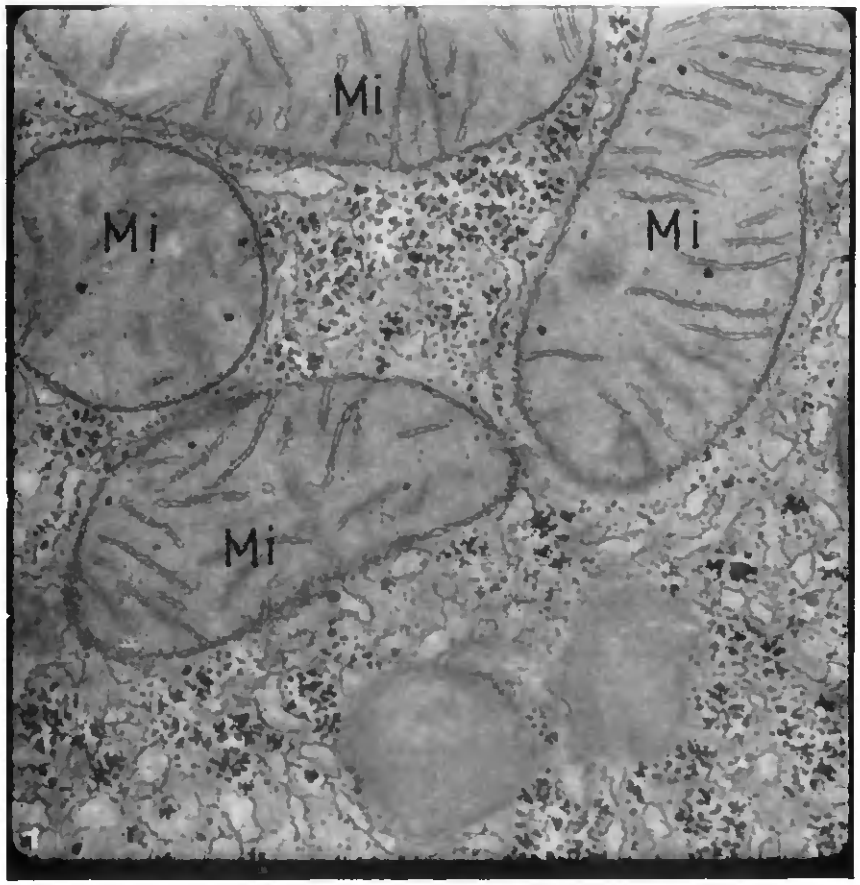

Fig. 1. Mitochondria (Mi) are corpuscles of variable shape, with a maximum dimension of about 1 μm. They have 2 membranes. The inner one is folded to form the cristae, within the organelle.

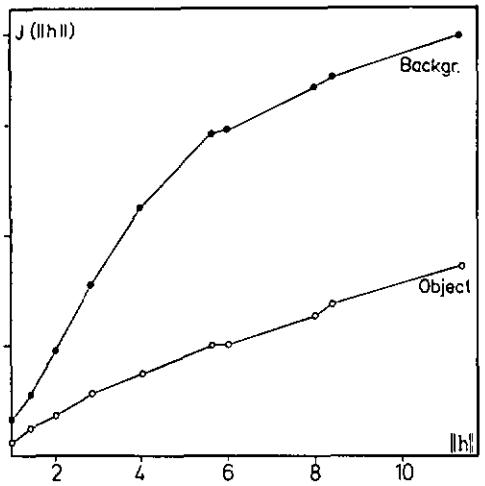

Fig. 2. The covariogram gives a measure of the correlation between grey values of neighbouring points. This measure increases as the correlation decreases and reaches the asymptotic value of the variance.

we found that smoothing could improve the result of Fig. 3. Figure 4 shows an example of what is obtained after smoothing. Further improvements can be made on the binary image: first eliminate small objects (Fig. 4e) in the background using their size as criterion, then suppress holes in the mitochondria using the closure (expand and shrink) operation. The final result is shown in Fig. 5.

The cristae, as well as the outer double membrane, are easily detectable. Their context is quite uniform: on both sides the substance is rather bright. The direction of the minimum of the grey-level function is to be found.

As the algorithm is to work inside the mitochondria only, these organelles, as detected by the previous algorithm, must be used as masks.

(b) *Results on a set of test images*

For the detection of mitochondria we compared the binary images obtained by the above-mentioned procedure with the drawing of a biologist for pictures that had not been used in the learning process.

The Bayesian error gave values between 10 and 15% with detection of texture. If one eliminates small objects and uses the closure these values decrease to 8%. This last value is a mean result taken over 10 pictures, the standard deviation beting 2.5%. Let us add that we have compared 2 specialists with the same test procedure. The mean error reached 5%.

Let us introduce

$$x = [i,j]$$

$$I(\lambda) = \begin{pmatrix} \lambda & 0 \\ 0 & \lambda \end{pmatrix}.$$

The logical expression

$$B(\lambda,\mu,x) = A[I(\lambda),0]x - [0,0] > \mu \quad \textit{and}$$
$$A[I(-\lambda),0]x - [0,0] > \mu$$

is true if and only if there is a valley in the image function of depth greater than μ and width less than, or equal to λ in a direction perpendicular to (i,j).

With the conditional expression:

$$E(\lambda,\mu,x) = \textit{ if } B(\lambda,\mu,x) \textit{ then } [0,0] \textit{ else } 0,$$

the image remains unchanged in the chosen valley and set to zero anywhere else.

In order to find valleys in several directions we use

$$v = [0,1], \quad d = [1,1] \quad \text{and} \quad R = \begin{pmatrix} 0 & -1 \\ 1 & 0 \end{pmatrix}$$

and we construct the expression

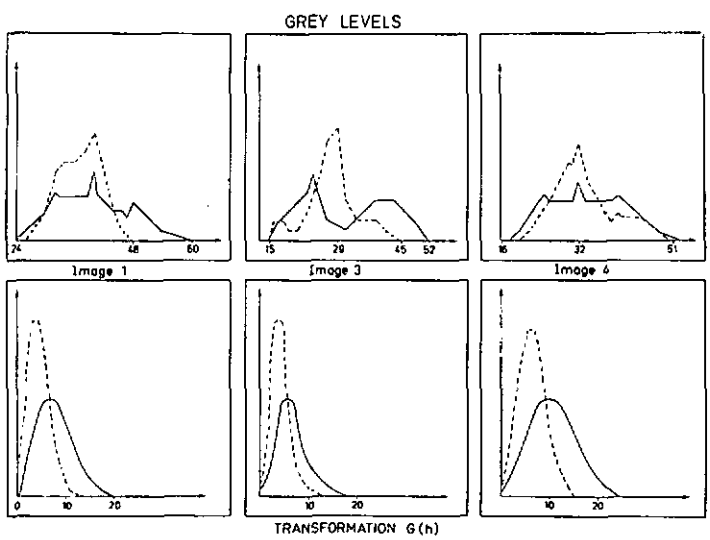

Fig. 3. Conditional grey-level distributions are plotted: full line for the background, dotted line for the object. The corresponding distribution of $G(h)$, for $h = 6$, is presented below. The transformation seems to reduce the variety of conditional grey-level distributions to one rather standard pattern.

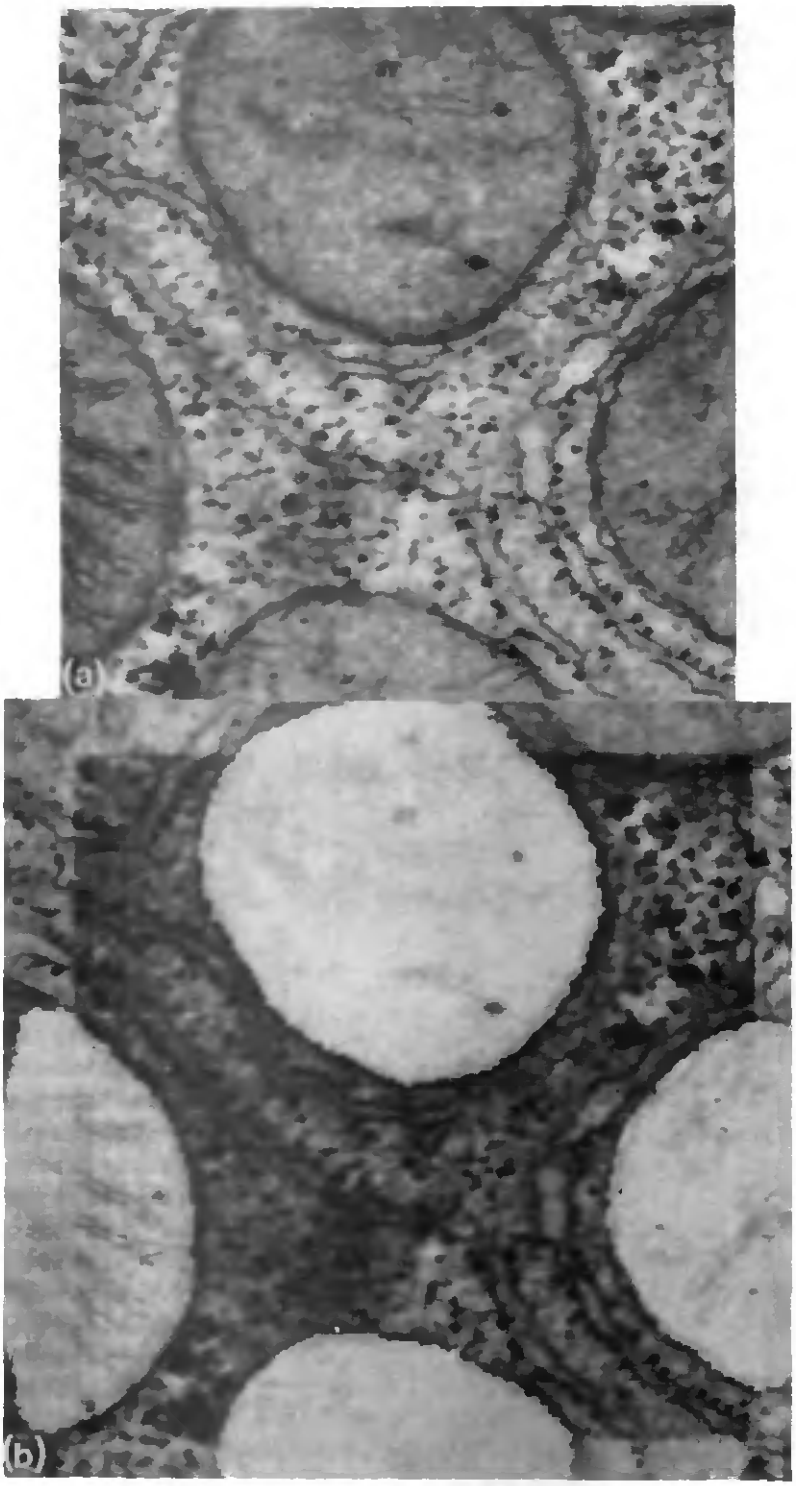

Fig. 4. (For caption see p. 183.)

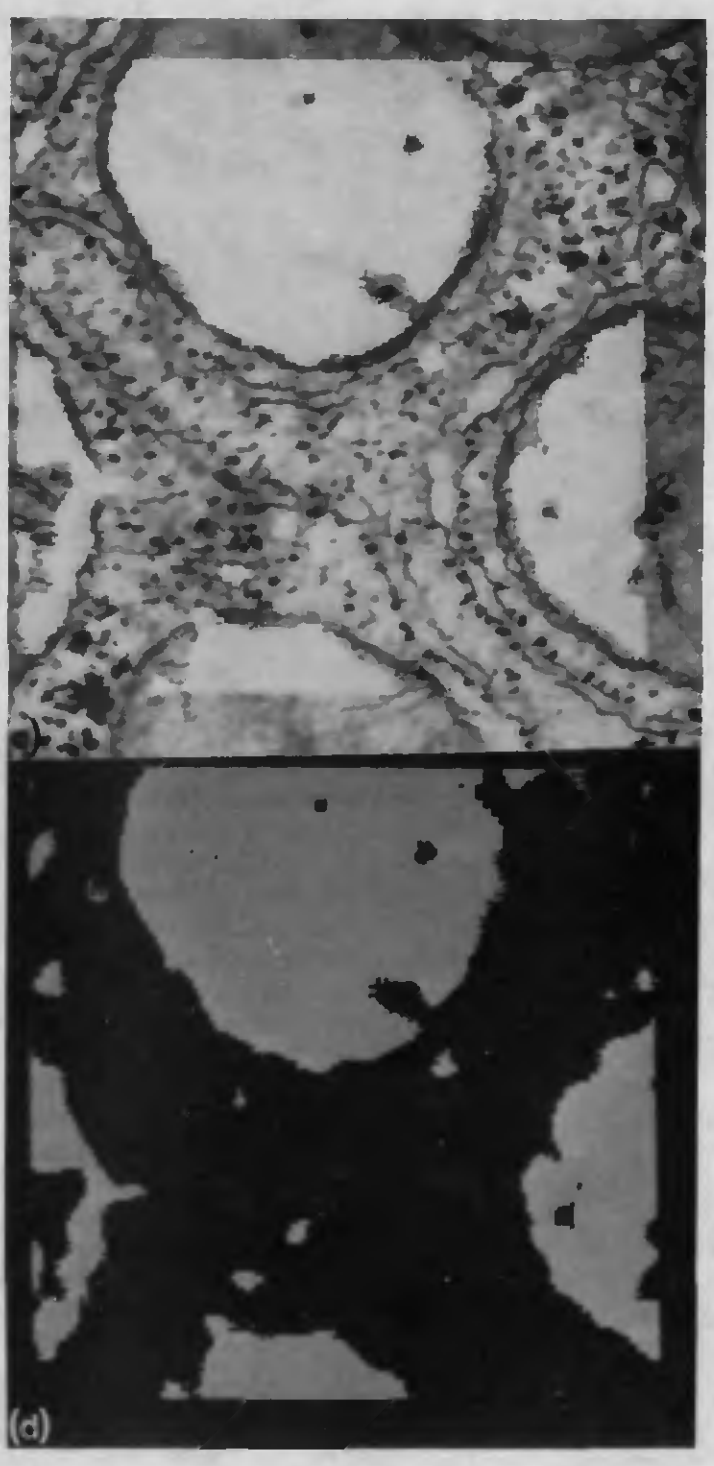

Fig. 4. (For caption see p. 183.)

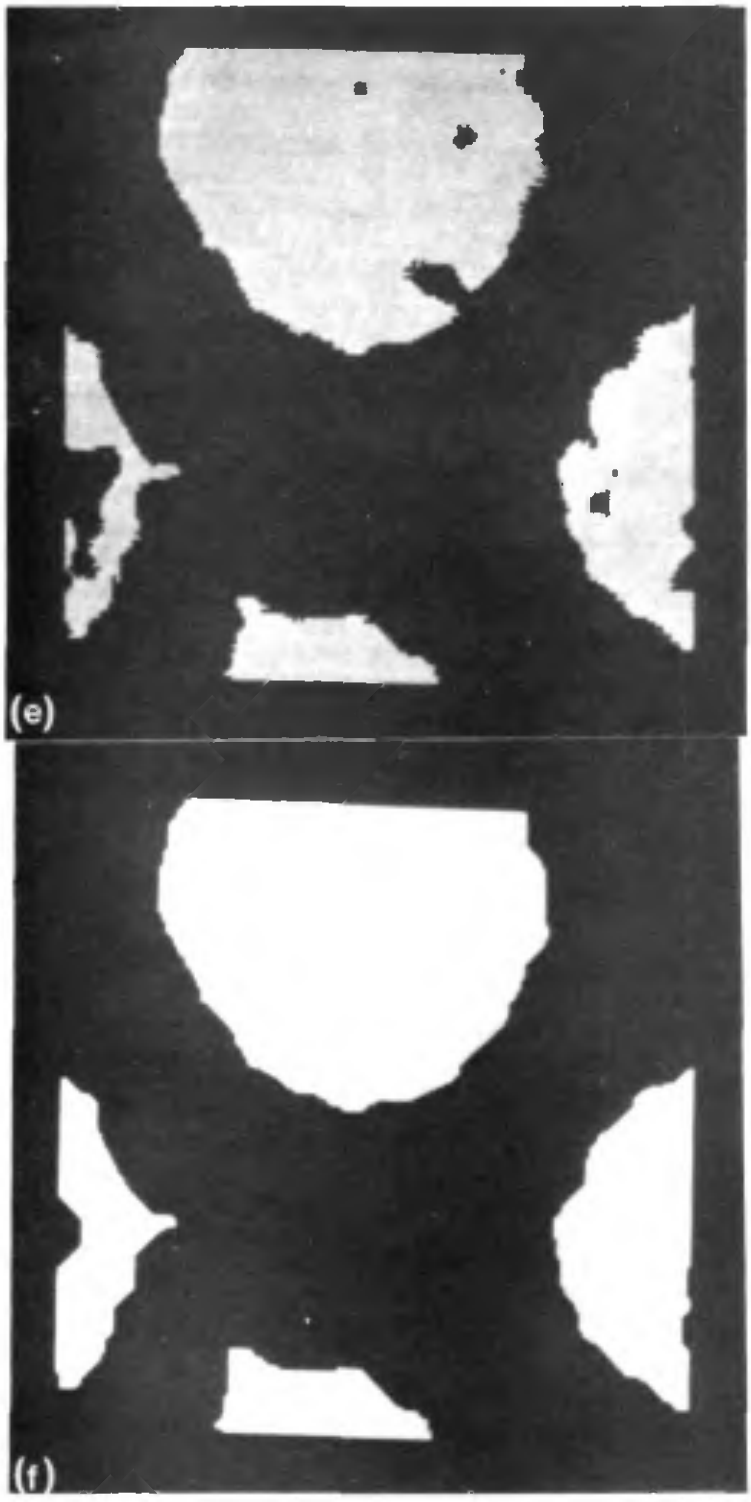

Fig. 4. These photographs show the different steps of the transformation performed to obtain a binary image that approaches the accuracy of a drawing by a specialist. (a) Original picture with the frame. (b) Hand drawing of mitochondria by a biologist, superimposed on original photomicrograph. (c) Texture detection. (d) The corresponding binary image. (e) The elimination of small objects. (f) The closure operation (expand and shrink).

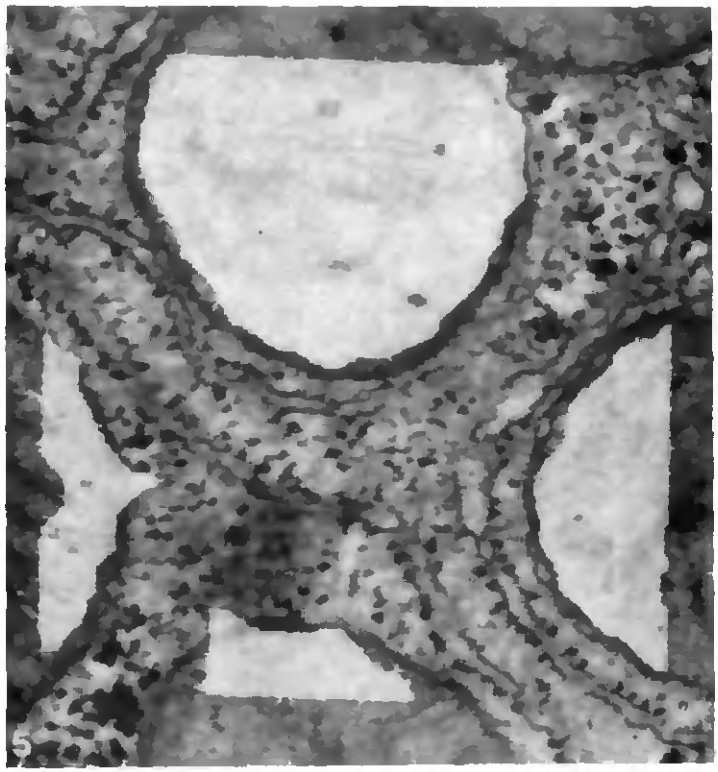

Fig. 5. The results, superimposed on original photomicrograph.

$$H(\lambda, \mu) = \text{Max}[E(\lambda, \mu, v), E(\lambda, \mu, d), A(R,0)E(\lambda, \mu, v), A(R,0)E(\lambda, \mu, d)].$$

This expression yields the results of Fig. 6 with suitable parameters λ, μ, the value of the latter depending on the picture's magnification. For membranes we used the second criterion mentioned above. The results were, on average, as follows: 80 per cent correctly detected membranes, 20 per cent incorrectly detected membranes, and 20 per cent of membranes undetected. Again we compared the results with those of 2 specialists and found them to be comparable.

CONCLUSIONS

The present application shows that local transformations of the initial image may reduce the object definition to a thresholding problem. The transformations have been helpful in texture discrimination as well as for local structure detection.

We observed that locally transforming the pictures tends to concentrate varying cases of grey level distributions (Fig. 3) into a standard pattern of conditional statistics. This means that information on the designed classification has been filtered on this type of picture.

Parameters of these transformations must be adjusted. The sampling distance between values used in the transformation depends on the magnification of the picture. The covariogram has proved to be useful in giving a quick estimate of this distance. Systematic trials have given the same result in a much longer time.

Accurate comparison of detected objects with those drawn by hand calls for criteria depending on their geometrical aspects. We have proposed a criterion to be used in the case of line-like objects and we have calculated the usual error of Bayes in the case of objects having a low form factor. It is worth noting that the accuracy of an estimate depends on the variatinn in the sample. A large variation of the geometric feature measured on the sampled objects will hide small defects in their detection.[10] It may therefore be luxurious to detect objects with a very high precision.

This kind of result based on local transforms seems encouraging, as it can be implemented on special hardware for local transforms, such as an array processor. The results of the present study have been used in the design of a programmable on-line processor to be included in our image analysis system.

SUMMARY

Efficient use of automatic image analysis equipment calls for automatic object definition with minimal user intervention. If object and background do not differ in their optical density, the common thresholding techniques break down; this is often the case with electron micrographs in biology. Among other local and global

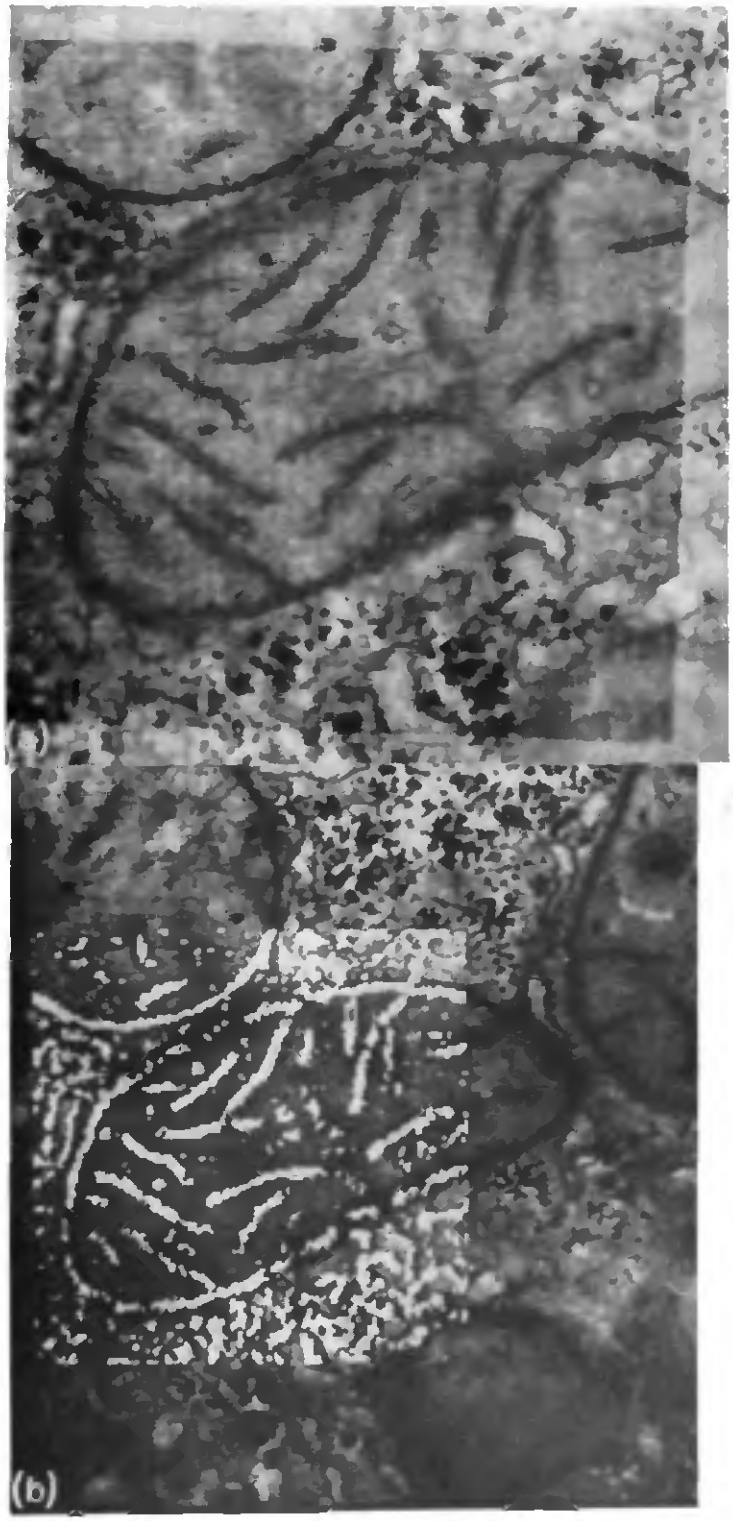

Fig. 6. (For caption see p. 187.)

Pattern Recognition, Vol. 13, No. 2, p. 189, 1981.
Printed in Great Britain

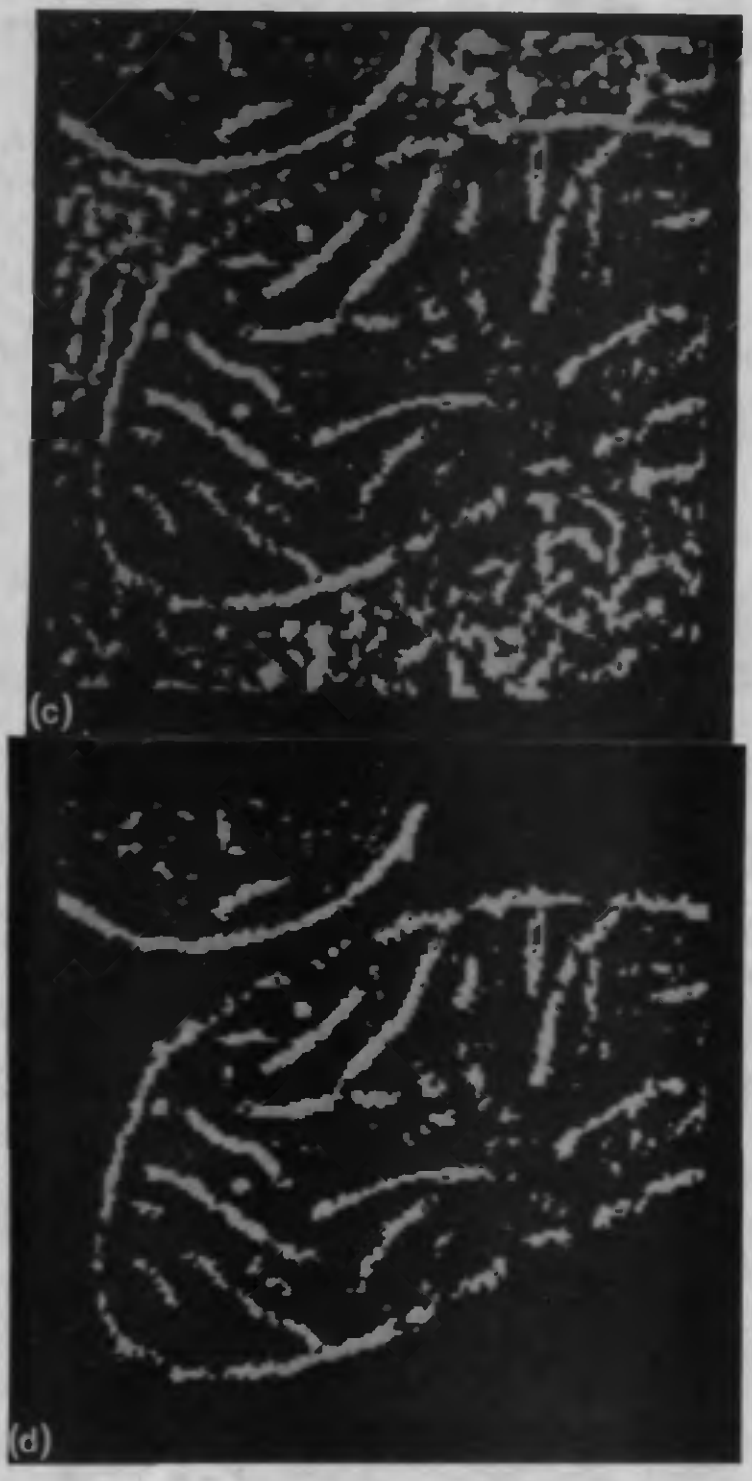

Fig. 6. (For caption see p. 187.)

Fig. 6. These figures show how to combine the preceding result with a local line detector to find the cristae and the membrane. (a) Original picture with the frame. (b) The local line detection. (c) The corresponding binary image. (d) The preceding result is used as a mask. (e) The result, superimposed on original photomicrograph.

descriptors, the observer uses texture for image segmentation.

In an attempt to simulate possible hardware extensions of our system, we have explored some local functions of grey level information. As a result, mitochondria of liver cells can be detected by using local grey level variations and by making simple corrections on the resulting binary image. Recognition of membranes has been achieved for the case of mitochondrial cristae.

REFERENCES

1. J. Serra, Lectures on image analysis by mathematical morphology. Cahier N-175 du Centre de Morphol. Math. de Fontainebleau, p. 4 (1976).
2. R. Duda and P. Hart, *Pattern Classification and Scene Analysis*, Wiley, New York (1973).
3. A. Rosenfeld, Y. Lee and R. Thomas, Edge and curve detection for texture discrimination. *Picture Processing and Psychopictorics*, A. P. (1976).
4. J. Weszka, C. Dyer and A. Rosenfeld, A comparative study of texture measures for terrain classification, *IEEE Trans. Syst. Man Cybernet.* **SMC-6**, 269–285 (1976).
5. A. Rosenfeld and M. Thurston, Edge and curve detection for visual scene analysis, *IEEE Trans. Comput.* **C-5**, 562–569 (1971).
6. R. M. Haralick, Automatic remote sensor image processing, *Digital Picture Analysis*, A. Rosenfeld, ed., pp. 47–52. Springer, Berlin (1976).
7. R. Duda and P. Hart, *Pattern Classification and Scene Analysis*, pp. 276–278. Wiley, New York (1973).
8. R. Duda and P. Hart, *Pattern Classification and Scene Analysis*, pp. 10–15. Wiley, New York (1973).
9. Z. Zucker, R. Hummel and A. Rosenfeld, An application of relaxation labelling to line and curve detection. *IEEE Trans. Comput.* **C-26**, 394–403 (1977).
10. O. Mathieu, L. M. Cruz-Orive, H. Hoppeler and E. R. Weibel. Measuring error and sampling variation in stereology, to be published in *J. Microsc.*

About the Author – HANSJOERG KELLER received his Ph.D. in physics in 1974 from the Institute of Applied Physics of the University of Berne. Since then he has directed a project on automated quantitative image analysis at the Institute of Anatomy, trying to combine hardware speed with software flexibility.

About the Author – ALAIN FAVRE joined the automatic image analysis group at the Institute of Anatomy with a diploma in applied mathematics. He contributed mainly to software and finished his Ph.D. on simulations of object detection by texture on electron micrographs in 1978. Since then he has worked on different segmentation techniques using local operators.